Broadband two-stage dynamic source inversion of 2016 Mw 6.2 Amatrice, Central Italy, earthquake

Ľubica Valentová K.* František Gallovič Sara Sgobba Francesca Pacor

Charles University, Prague, Czech Republic INGV Milan, Italy

I. Goal and motivation

- Obtain (broadband) dynamic source model of Mw6.2 Amatrice earthquake by combining low-frequency waveform dynamic source inversion with dynamic source inversion of apparent spectra in broad-frequency range in a multi-stage approach.
- In the first stage, the dynamic source inversion of waveforms is performed in the low-frequency range (up to 0.5-1Hz) and results in smooth dynamic models. These models are depleted in the higher-frequency content.
- In the second stage, the dynamic source inversion is applied to the so-called apparent source spectra: in ground-motion modeling community, the observed spectra are decomposed into source, path and site term. The extracted source spectra are cleaned from path and site effects so it is not necessary to simulate the source-to-site propagation. In addition, the source spectra are recovered over a large set of stations.
- The second stage of the inversion is performed in the complementary frequency range (the apparent spectra are estimated in frequencies above 0.5 Hz).
- The second stage of the inversion does not compromise the long-scale rupture properties of the first-stage model. The first-stage dynamic model can be used as a starting model of the second stage.
- The resulting broadband dynamic model contains long-scale properties constrained by the waveform inversion and is enriched at higher-frequencies by the second-stage inversion, still controlled by the observations.

II. Method

Dynamic rupture code FD3D_TSN (Premus et al., 2020)

- 4th order finite differences in a Cartesian box (Madariaga et al., 1998)
- Vertical fault in 1D layered velocity model
- Friction law implemented by traction-at-split-node method (Dalguer and Day, 2007)
- Symmetry conditions: problem solved on half of the domain, PML nonreflecting boundaries
- Ported to GPU using ACC directives - up to 10x faster than CPU
- Validated against SCEC community benchmarks with heterogeneous dynamic parameters
- Freely available on github: https://github.com/fgallovic/fd3d_tsn_pt

Bayesian inversion (Gallovič et al., 2019a)

- Markov chain Monte Carlo sampling by the Parallel tempering method (Sambridge, 2013)
- Prior constraints: M_0 with uncertainty, weak nucleation around prescribed hypocenter (<1 MPa), nonnegative friction drop and prestress, D_c >15 mm
- Assuming Gaussian data errors to calculate misfit

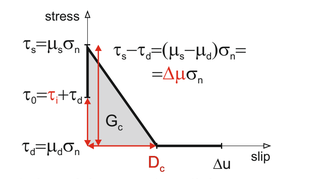

Inverted model parameters (inhomogeneous along the fault):
- Friction drop $\Delta\mu$ (static - dynamic friction coefficient)
- Characteristic slip-weakening distance D_c
- Initial stress τ_i

III. Data

Stage 1: Low-frequency waveforms

- Records of 38 stations within 50km distance from source
- Accelerations integrated to displacements
- Band-pass filtered 0.05-0.5Hz except for 3 nearest stations (AMT,NRC,NOR) which were filtered 0.05-1Hz.
- Downloaded from ESM database (`https://esm-db.eu/#/event/EMSC-20160824_0000006`)

Stage 2: Apparent source spectra

- Decomposition of acceleration S-wave amplitude spectra A_{ij} at station j for event i:
  $\log_{10} A_{ij}(f) = \log_{10} S_{ij}(f, M_i) + \log_{10} P_{ij}(f, r_{ij}) + \log_{10} G_j(f)$
  where S_{ij} corresponds to apparent source spectra of event i at station j, P_{ij} is an attenuation function comprising geometrical spreading and frequency-dependent attenuation, and $G_j(f)$ is the site response at station j
- Decomposition performed over large number of events in Central Italy and stations using the so-called generalized inversion technique (GIT, Bindi et al., 2009; Pacor et al.,2016; Oth et al., 2008; `https://shake.mi.ingv.it/central-italy/`
- Apparent spectra at 131 stations in frequency range 0.5-4.5 Hz

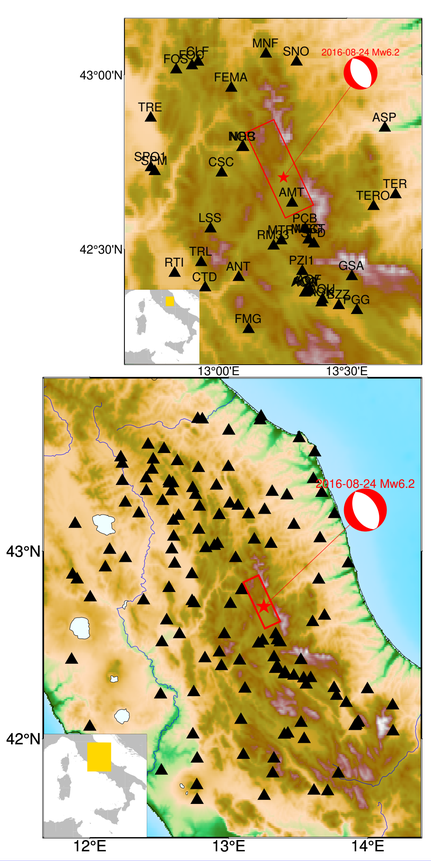

IV. Stage 1: Low-frequency waveform inversion of Mw 6.2 Amatrice

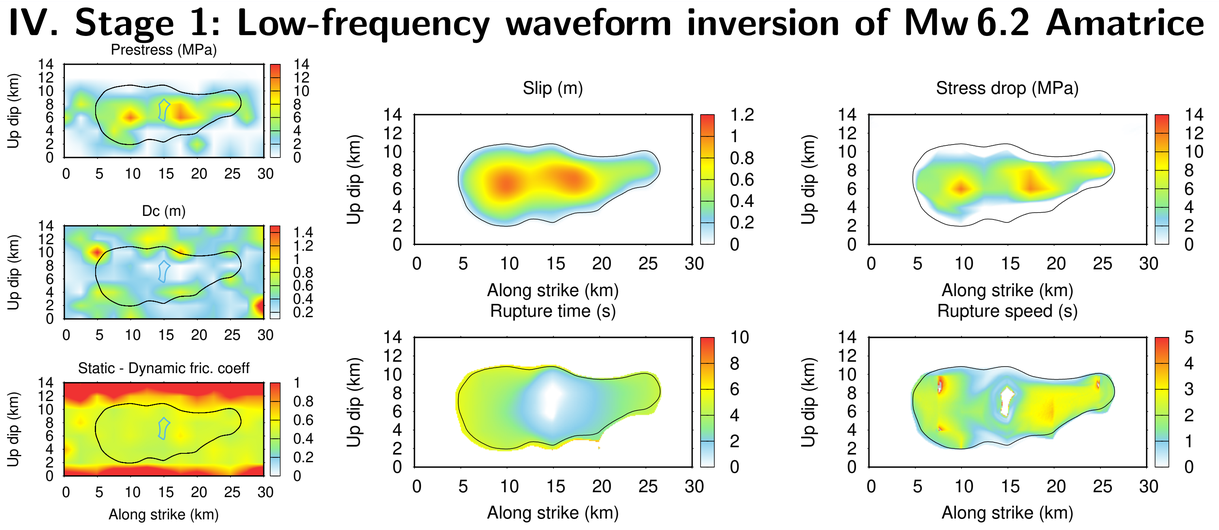

Stage-1 model: dynamic source parameters and resulting kinematic model of the maximum a posterior (MAP) model of the low-frequency waveform inversion.

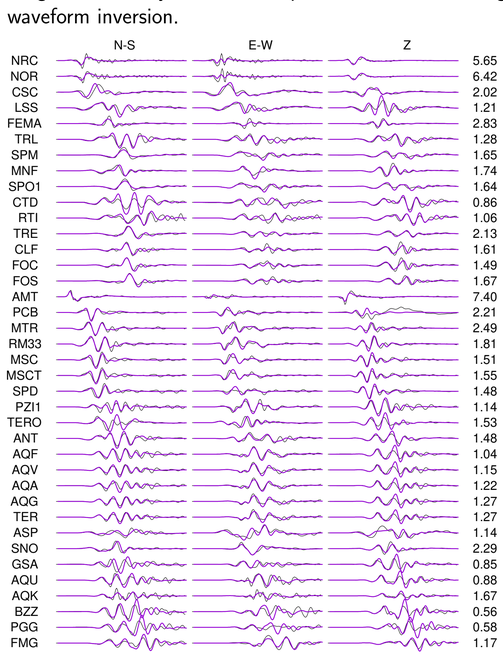

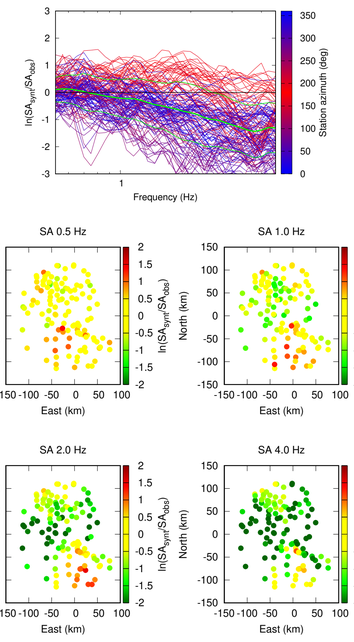

Left: Low-frequency (up to 0.5-1 Hz) waveform fit over 38 stations of the Stage-1 model. Variance reduction is 55%.
Right: Spectral bias between simulated and observed apparent source spectra of the Stage-1 model over 131 stations as a function of frequency and in map view for selected frequencies. Mean spectral bias (over stations and frequencies) is -0.71.
The underestimation of the synthetic source spectra of the smooth Stage-1 model at higher frequencies is present over a wide range of azimuth and distances (except for strong directivity to south).

V. Stage 2: Broadband inversion of apparent source spectra of Mw 6.2 Amatrice

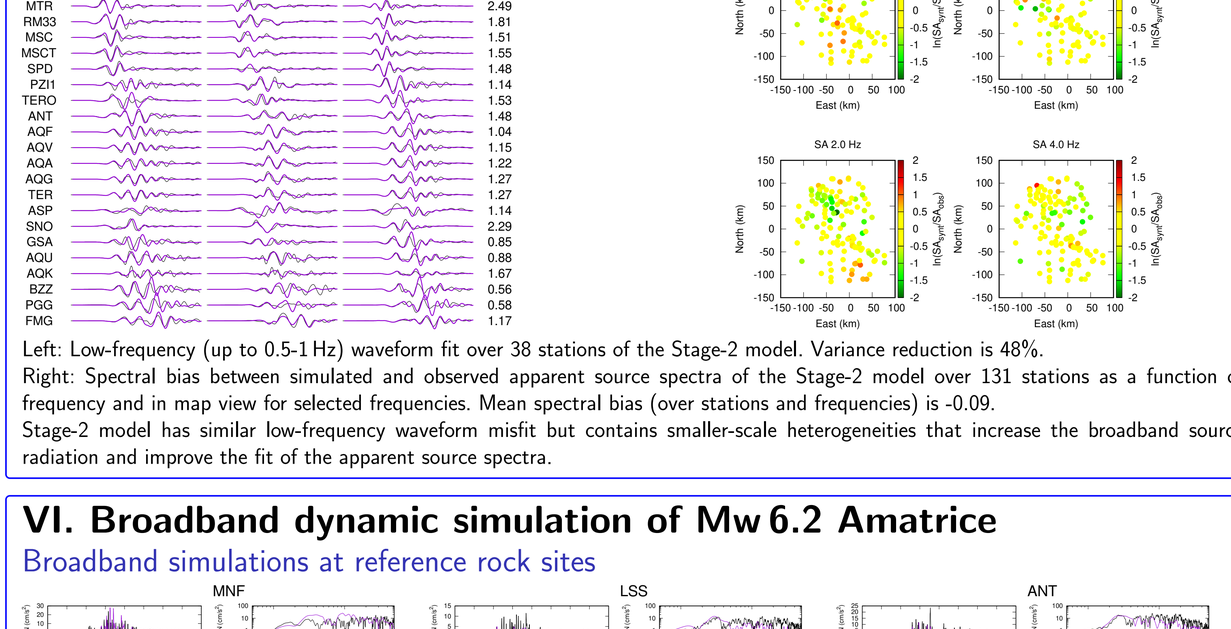

Stage-2 model: dynamic source parameters and resulting kinematic model of MAP model of the broadband (0.5-4.5 Hz) apparent spectra inversion.

Left: Low-frequency (up to 0.5-1 Hz) waveform fit over 38 stations of the Stage-2 model. Variance reduction is 48%.
Right: Spectral bias between simulated and observed apparent source spectra of the Stage-2 model over 131 stations as a function of frequency and in map view for selected frequencies. Mean spectral bias (over stations and frequencies) is -0.09.
Stage-2 model has similar low-frequency waveform misfit but contains smaller-scale heterogeneities that increase the broadband source radiation and improve the fit of the apparent source spectra.

VI. Broadband dynamic simulation of Mw 6.2 Amatrice

Broadband simulations at reference rock sites

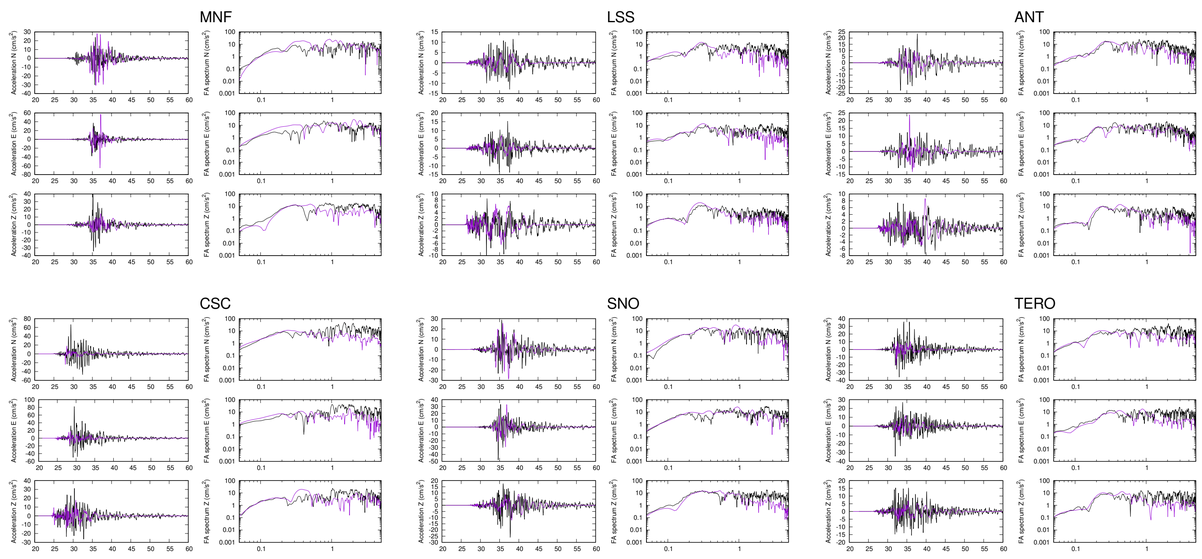

Synthetic acceleration waveforms (filtered 0.05-4.5Hz) (simulated using Stage-2 dynamic model at rock-site velocity model) and their Fourier amplitude (FA) spectra compared with observations, example at 6 reference rock stations. Althought the high-frequency content is improved, the underestimation at highest frequencies is still present.

Broadband simulations at non-reference sites

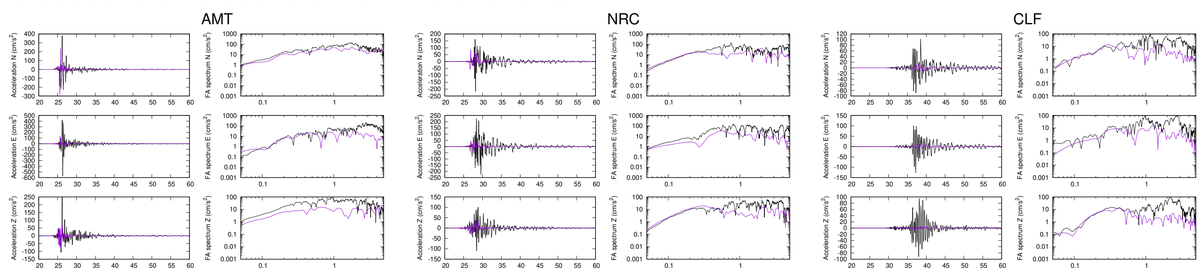

Synthetic acceleration waveforms (filtered 0.05-4.5Hz) (simulated using Stage-2 dynamic model at rock-site velocity model) and their FA spectra compared with observations, example at two near-fault stations AMT and NRC and a station with significant site effects CLF.

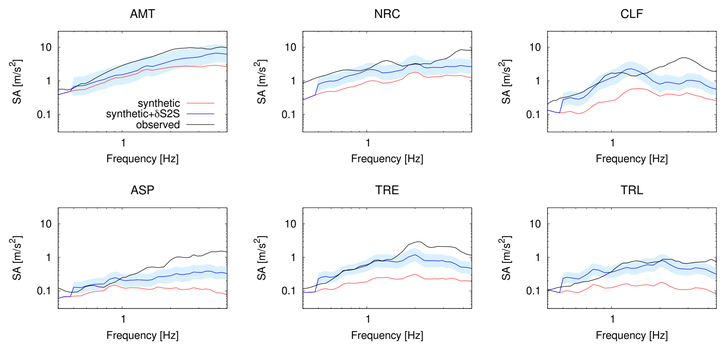

Synthetic response spectral accelerations (SA) at non-reference stations with various station azimuth calculated using rock-site velocity model (red), and SA corrected (blue) by empirical site-effect evaluated as $\delta S2S$ in ground motion model of Central Italy by Sgobba et al. (2021). Blue shaded region marks the uncertainty of the site correction in terms of $\pm$ 1 standard deviation. Black curves show the observed SAs.

Applying station corrections helps to explain observed SAs at stations AMT, NRC, TRL, but the corrected-synthetic SAs still lack at higher frequencies at other stations. This may result from i) complex 3D geology below the station unaccounted in the site correction function (e.g., CLF located in a sedimentary basin); ii) unmodeled source effect (e.g., weaker directivity towards north); or combination of both. The latter effect should be recovered by the apparent spectra inversion. Stage-2 inversion is still running.

The broadband source inversion is computationally very expensive:

- model grid spacing is 500 m, leading to ∼7500 model parameters
- FD3D simulation uses 50 m spatial grid and 0.5 ms temporal grid

References

Bindi, D., Pacor, F., Luzi, L., Massa, M., Ameri, G. (2009). The Mw 6.3, 2009 L'Aquila earthquake: source, path and site effects from spectral analysis of strong motion data, *Geophys. J. Int.*, 179(3), 1573–1579.

Dalguer, L. A., & Day, S. M. (2007). Staggered-grid split-node method for spontaneous rupture simulation. *J. Geophys. Res.*, 112(B2), B02302.

Gallovič, F., Valentová, Ľ., Ampuero, J.-P., Gabriel, A.-A. (2019a). Bayesian Dynamic Finite-Fault Inversion: 1. Method and Synthetic Test, *J. Geophys. Res. Solid Earth* 124, 6949-6969.

Gallovič, F., Valentová, Ľ., Ampuero, J.-P., Gabriel, A.-A. (2019b). Bayesian Dynamic Finite-Fault Inversion: 2. Application to the 2016 Mw6.2 Amatrice, Italy, Earthquake, *J. Geophys. Res. Solid Earth* 124, 6970-6988.

Madariaga, R., Olsen, K. B., & Archuleta, R. J. (1998). Modelling dynamic rupture in a 3D earthquake fault model. *Bull. Seismol. Soc. Am.*, 88(5), 1182–1197.

Oth, A., Bindi, D., Parolai, S., Wenzel, F. (2008). S-wave attenuation characteristics beneath the Vrancea region in Romania: new insights from the inversion of ground-motion spectra, *Bull. Seism. Soc. Am.*, 98(5), 2482–2497.

Pacor, F., Spallarossa, D., Oth, A., Luzi, L., Puglia, R., Cantore, L., Mercuri, A., D'Amico, M., Bindi, D. (2016). Spectral models for ground motion prediction in the L'Aquila region (central Italy): evidence for stress-drop dependence on magnitude and depth, *Geophys. J. Int.* 204(2) 697–718.

Premus, J., Gallovič, F., Hanyk, L., Gabriel, A.-A. (2020). FD3D_TSN: Fast and simple code for dynamic rupture simulations with GPU acceleration, *Seism. Res. Lett.* 91, 2881-2889.

Sambridge, M. (2013). A Parallel Tempering algorithm for probabilistic sampling and multimodal optimization. *Geophys. J. Int.*, 196, 357–374.

Sgobba, S., Lanzano, G., Pacor, F. (2021). Empirical nonergodic shaking scenarios based on spatial correlation models: An application to central Italy, *Earthq. Eng. Struct. Dynam.* 50, no. 1, 60–80.

*Contact: `valent@karel.troja.mff.cuni.cz`